Synthesis, Structural Investigation and Characterization of an α-Keggin-based Organic-Inorganic Hybrid, $[Cu(BIIM)_2]\{[Cu(BIIM)_2(H_2O)][Cu(BIIM)_2BW_{12}O_{40}]\cdot 3H_2O\}_2$ (BIIM = 2,2′-Biimidazole)

Lin-Heng Wei[a], Zi-Liang Wang[b] and Ming-Xue Li[a]

[a] Institute of Natural Resources and Environmental Science, College of Environment and Planning, Henan University, Kaifeng 475001, P. R. China

[b] College of Chemistry and Chemical Engineering, Henan University, Kaifeng 475001, P. R. China

Reprint requests to Lin-Heng Wei. E-mail: linhengw@henu.edu.cn or Zi-Liang Wang. E-mail: zlwang@henu.edu.cn

Z. Naturforsch. **2013**, *68b*, 1219 – 1224 / DOI: 10.5560/ZNB.2013-3116
Received April 14, 2013

An organic-inorganic hybrid based on the α-Keggin anion $[BW_{12}O_{40}]^{5-}$, $[Cu(BIIM)_2]\{[Cu(BIIM)_2(H_2O)][Cu(BIIM)_2BW_{12}O_{40}]\cdot 3H_2O\}_2$ (BIIM = 2,2′-biimidazole) (**1**) was hydrothermally prepared and characterized by elemental analysis, IR and UV spectra. Compound **1** is composed of $[Cu(BIIM)_2]^{2+}$ and $[Cu(BIIM)_2(H_2O)]^{2+}$ cations and a $[Cu(BIIM)_2BW_{12}O_{40}]^{3-}$ polyanion, in which the $[BW_{12}O_{40}]^{5-}$ anion is decorated by one $[Cu(BIIM)_2]^{2+}$ cation through one terminal oxygen atom. These components are finally arranged through hydrogen bonds into a two-dimensional network. Investigations of the intermolecular interactions by Hirshfeld surface and fingerprint plots indicate that besides the classical N–H···O hydrogen bonds, there are rare W–O(terminal)···π(imidazole ring) interactions stabilizing the structure.

Key words: Crystal Structure, Copper(II), Keggin, Hirshfeld Surface, Fingerprint Plots

Introduction

Design and syntheses of novel hybrids based on polyoxometalates have been attracting great interest due to their various architectures and potential applications in chemistry, physics and material science [1 – 7]. Polyoxometalates may have different reactivity in coordinating to metal ions and their introduction into hybrids as inorganic units is an important breakthrough in preparing hybrid materials, which greatly give impetus to the rapid developments of this field.

Saturated POMs, namely, XM_{12} $\{[PM_{12}O_{40}]^{3-}$ (M = Mo, W) [8 – 15], $[XM_{12}O_{40}]^{4-}$ (X = Si, Ge; M = Mo, W) [16 – 21]$\}$ have higher negative charges and high symmetry and are stable in a broad pH range. However, compared with $[PM_{12}O_{40}]^{3-}$ and $[XM_{12}O_{40}]^{4-}$ anions, hybrids based on the α-Keggin-type $[BW_{12}O_{40}]^{5-}$ [22 – 25] anions with a smaller radius of boron are less common. The $[BW_{12}O_{40}]^{5-}$ anion generally can act as a charge-compensating or space-filling constituent [24]. Secondly, the $[BW_{12}O_{40}]^{5-}$ anion acts as an inorganic building block attached to a transition metal site of complex cations forming isolated, or one- and multi-dimensional structures [25]. The functions of $[BW_{12}O_{40}]^{5-}$ polyanions are determined by the reaction conditions, such as, among others, metal to ligand ratio, temperature, and starting pH value.

As a continuation of our study [26, 27], 2,2′-biimidazole (BIIM) has been selected as ligand to Cu(II) because it possesses two nitrogen coordination sites and two -NH donor functions. For hydrogen bonding compounds built with 2,2′-biimidazole are not frequent [28]. Herein we present the synthesis, structural analysis and characterization of an α-Keggin-based organic-inorganic hybrid, $[Cu(BIIM)_2]\{[Cu(BIIM)_2(H_2O)][Cu(BIIM)_2BW_{12}O_{40}]\cdot 3H_2O\}_2$ (**1**).

Experimental Section

General

All chemicals were of reagent grade as received from commercial sources and used without further purification. C, H, N elemental analyses were performed on a Perkin-Elmer 240C elemental analyzer. The infrared spectrum was recorded from KBr pellets on a Nicolet 170SXFT-IR spectrometer in the range of 400 – 4000 cm^{-1}. The UV spectrum was obtained on a Shimzu UV-250 spectrometer in the range 190 – 400 nm.

*Synthesis of [Cu(BIIM)$_2$]{[Cu(BIIM)$_2$(H$_2$O)][Cu(BIIM)$_2$BW$_{12}$O$_{40}$]·3H$_2$O}$_2$ (**1**)*

A mixture of $Na_2WO_4 \cdot 2H_2O$ (0.50 g, 1.5 mmol), $Na_2B_4O_7 \cdot 4H_2O$ (0.05 g, 0.13 mmol), $CuCl_2 \cdot 2H_2O$ (0.07 g, 0.42 mmol), $Cu(CH_3COO)_2 \cdot H_2O$ (0.10 g, 0.48 mmol), BIIM (0.03 g, 0.13 mmol), and H_2O (15 mL) was sealed in a Teflon-lined stainless-steel reactor and heated at 160 °C for 4 d with a starting pH = 4 adjusted with hydrochloric acid (6 mol L^{-1}). After cooling slowly to room temperature within about 24 h, blue crystals were obtained with 16.6 % yield on tungsten basis. – Elemental analysis: calcd. C 9.59, H 1.02, N 7.45; found C 9.47, H 1.07, N, 7.35. – IR (cm^{-1}): ν = 3258 (w), 3171(w), 2927(w), 1620(w), 1536(m), 1425(m), 1000(w), 953(m), 906(m), 823(s), 755(w).

Crystal structure determination

The data collection was performed on a Bruker SMART APEX CCD area-detector diffractometer using graphite-monochromatized MoK_α radiation (λ = 0.71073 Å) at 293(2) K. The intensities were corrected for Lorentz and polarization effects and empirically for absorption. The structure was solved by Direct Methods and refined by full-matrix least-squares techniques based on F^2 using the SHELXS-97 and SHELXL-97 [29] programs, respectively. All non-hydrogen atoms were refined anisotropically. For the polyoxometalate system, H atoms bound to water are very difficult to locate in the difference Fourier maps so that they were omitted from the final model. All remaining H atoms were positioned geometrically. The structure evaluation was done with PLATON [30]. Crystal data and structure refinements are summarized in Table 1. Selected bond lengths and angles are given in Table 2.

CCDC 922709 contains the supplementary crystallographic data for this paper. These data can be obtained free of charge from The Cambridge Crystallographic Data Centre *via* www.ccdc.com.ac.uk/data_request/cif.

Table 1. Crystallographic data for [Cu(BIIM)$_2$]{[Cu(BIIM)$_2$(H$_2$O)][Cu(BIIM)$_2$BW$_{12}$O$_{40}$]·3H$_2$O}$_2$ (**1**).

Empirical formula	$C_{60}H_{76}B_2Cu_5N_{40}O_{88}W_{24}$
M_r	7517.22
Crystal size, mm^3	0.17 × 0.13 × 0.11
Crystal system	triclinic
Space group	$P\bar{1}$
a, Å	11.3750(14)
b, Å	12.8930(16)
c, Å	22.329(3)
α, deg	92.2550(18)
β, deg	92.309(2)
γ, deg	90.876(2)
V, $Å^3$	3269.1(7)
Z	1
$D_{calcd.}$, g cm^{-3}	3.81
μ(MoK_α), mm^{-1}	21.9
F(000), e	3335
Refl. measured/unique/R_{int}	18 469/12 714/0.0311
Param. refined	988
$R1/wR2$ [$I > 2\,\sigma(I)$][a]	0.0379/0.0805
$R1/wR2$ (all data)[a]	0.0526/0.0860
GoF (F^2)[b]	0.977
$\Delta\rho_{fin}$ (max/min) e $Å^{-3}$	1.97/−2.16

[a] $R1 = \Sigma||F_o| - |F_c||/\Sigma|F_o|$; $wR2 = [\Sigma w(F_o^2 - F_c^2)^2/\Sigma w(F_o^2)^2]^{1/2}$, $w = [\sigma^2(F_o^2) + (0.0332P)^2]^{-1}$, where $P = (\mathrm{Max}(F_o^2, 0) + 2F_c^2)/3$; [b] GoF $= [\Sigma w(F_o^2 - F_c^2)^2/(n_{obs} - n_{param})]^{1/2}$.

Results and Discussion

*Crystal structure of [Cu(BIIM)$_2$]{[Cu(BIIM)$_2$(H$_2$O)][Cu(BIIM)$_2$BW$_{12}$O$_{40}$]·3H$_2$O}$_2$ (**1**)*

Complex **1** belongs to the triclinic crystal system, space group $P\bar{1}$ with $Z = 1$, consisting of two $[Cu(BIIM)_2BW_{12}O_{40}]^{3-}$ polyanions, two $[Cu(BIIM)_2(H_2O)]^{2+}$ cations, six water molecules and one isolated $[Cu(BIIM)_2]^{2+}$ cation in which the Cu^{2+} site is situated on an inversion center (Fig. 1). In the $[Cu(1)(BIIM)_2BW_{12}O_{40}]^{3-}$ polyanion, the $[BW_{12}O_{40}]^{5-}$ anion is decorated by a $[Cu(1)(BIIM)_2]^{2+}$ ion through one terminal oxygen O(1) atom. The Cu(1)-centered square pyramid is defined by four N atoms from two BIIM ligands in the basal plane and an apical oxygen atom bridging to a WO_6 octahedron with a Cu(1)−O distance of 2.349(7) Å and Cu(1)−N bond lengths in the range of 1.995(9) – 2.020(9) Å. The coordination environment of the Cu(2) site is similar to that of Cu(1), but the apical oxygen position is occupied by a water molecule with a Cu(2)−O(1W) bond length of 2.272(8) and Cu(2)−N distances varying from 2.008(9) to

Table 2. Selected bond lengths (Å) and angles (deg) of **1**[a].

Cu(1)–N(2)	1.995(9)	Cu(2)–N(9)	2.008(9)
Cu(1)–N(1)	1.997(10)	Cu(2)–N(10)	2.020(9)
Cu(1)–N(6)	2.015(8)	Cu(2)–N(13)	2.022(9)
Cu(1)–N(5)	2.020(9)	Cu(2)–N(14)	2.024(10)
Cu(1)–O(1)	2.349(7)	Cu(2)–O(1W)	2.272(8)
Cu(3)–N(17)	1.963(9)	Cu(3)–N(18)	1.986(9)
Cu(3)–N(17)#1	1.963(9)	Cu(3)–N(18)#1	1.986(9)
B(1)–O(37)	1.534(12)	B(1)–O(39)	1.564(12)
B(1)–O(40)	1.545(13)	B(1)–O(38)	1.567(12)
W(1)–O(1)	1.711(7)	W(2)–O(2)	1.702(7)
W(3)–O(3)	1.703(7)	W(4)–O(4)	1.693(7)
W(5)–O(5)	1.713(7)	W(6)–O(6)	1.735(7)
W(7)–O(7)	1.701(8)	W(8)–O(8)	1.690(7)
W(9)–O(9)	1.702(7)	W(10)–O(10)	1.719(7)
W(11)–O(11)	1.699(8)	W(12)–O(12)	1.706(7)
N(2)–Cu(1)–N(1)	81.7(4)	N(6)–Cu(1)–N(5)	83.3(4)
N(2)–Cu(1)–N(6)	162.7(4)	N(2)–Cu(1)–O(1)	114.9(4)
N(1)–Cu(1)–N(6)	98.0(4)	N(1)–Cu(1)–O(1)	93.6(4)
N(2)–Cu(1)–N(5)	96.6(4)	N(6)–Cu(1)–O(1)	82.3(3)
N(1)–Cu(1)–N(5)	177.9(4)	N(5)–Cu(1)–O(1)	88.2(3)
N(9)–Cu(2)–N(10)	81.8(4)	N(13)–Cu(2)–N(14)	82.0(4)
N(9)–Cu(2)–N(13)	168.6(4)	N(9)–Cu(2)–O(1W)	95.7(3)
N(10)–Cu(2)–N(13)	97.7(4)	N(10)–Cu(2)–O(1W)	100.9(4)
N(9)–Cu(2)–N(14)	95.8(4)	N(13)–Cu(2)–O(1W)	95.5(4)
N(10)–Cu(2)–N(14)	166.4(4)	N(14)–Cu(2)–O(1W)	92.7(4)
N(17)–Cu(3)–N(17)#1	180	N(17)–Cu(3)–N(18)#1	97.2(4)
N(17)–Cu(3)–N(18)	82.8(4)	N(17)#1–Cu(3)–N(18)#1	82.8(4)
N(17)#1–Cu(3)–N(18)	97.2(4)	N(18)–Cu(3)–N(18)#1	180
O(37)–B(1)–O(40)	110.5(8)	O(37)–B(1)–O(38)	111.6(7)
O(37)–B(1)–O(39)	109.3(8)	O(40)–B(1)–O(38)	109.1(8)
O(40)–B(1)–O(39)	109.2(7)	O(39)–B(1)–O(38)	107.1(7)

[a] Symmetry transformations used to generate equivalent atoms: #1 $-x+1, -y+1, -z$.

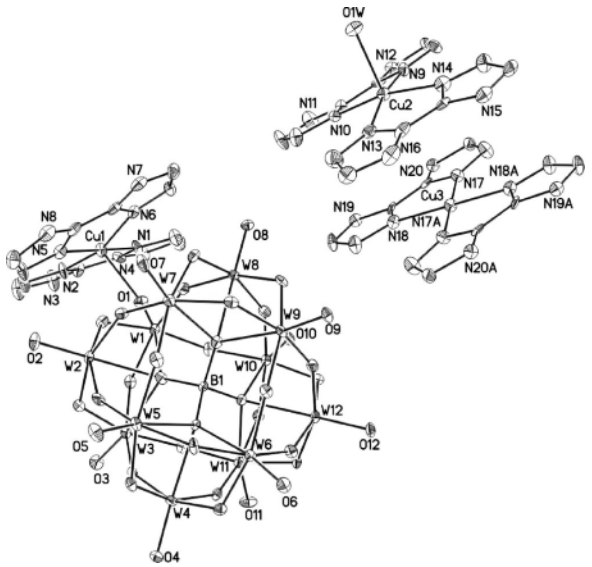

Fig. 1. Unit of **1** showing the atom-numbering scheme adopted. Displacement ellipsoids are drawn at the 30 % probability level. The discrete water molecules, hydrogen atoms attached to carbon and nitrogen atoms are omitted for clarity.

2.024(10) Å. The Cu(3) site is square planar with four N atoms from two BIIM ligands with Cu(3)−N distances 1.963(9) – 1.986(9) Å. The $[BW_{12}O_{40}]^{5-}$ anion has the following distances: W–O_t, 1.690(7) – 1.735(7) Å, W-$O_{b,c}$ 1.858(8) – 1.958(7) Å and W–O_a 2.290(7) – 2.429(6) Å. For the BO_4 tetrahedron, the B–O distances are in the range of 1.534(12) – 1.567(12) Å with an average length of 1.522 Å, while the O–B–O angles vary from 107.1(7) to 111.6(7)°. Compared to the Cu(2)N_4O square pyramid, it is clear that the Cu(1)N_4O square pyramid is distinctly elongated along the Cu–O–W axis due to the O(1)–W bridge. Additionally, WO_6 octahedra and BO_4 tetrahedra are slightly distorted, affected by the $[Cu(BIIM)_2]^{2+}$ cations.

The BIIM ligand also interacts with the $[BW_{12}O_{40}]^{5-}$ anion *via* hydrogen bonds. For the $[Cu(1)(BIIM)_2]^{2+}$ ion at (x, y, z), N(3)–H and N(4)–H as donors link to O(13) ($-x$, $-y+1$, $-z+1$) and O(16) ($-x$, $-y+1$, $-z+1$), and N(7)–H and N(8)–H interact with O(3W) (x, y, z) and O(2) ($-x+1$, $-y$, $1-z$),

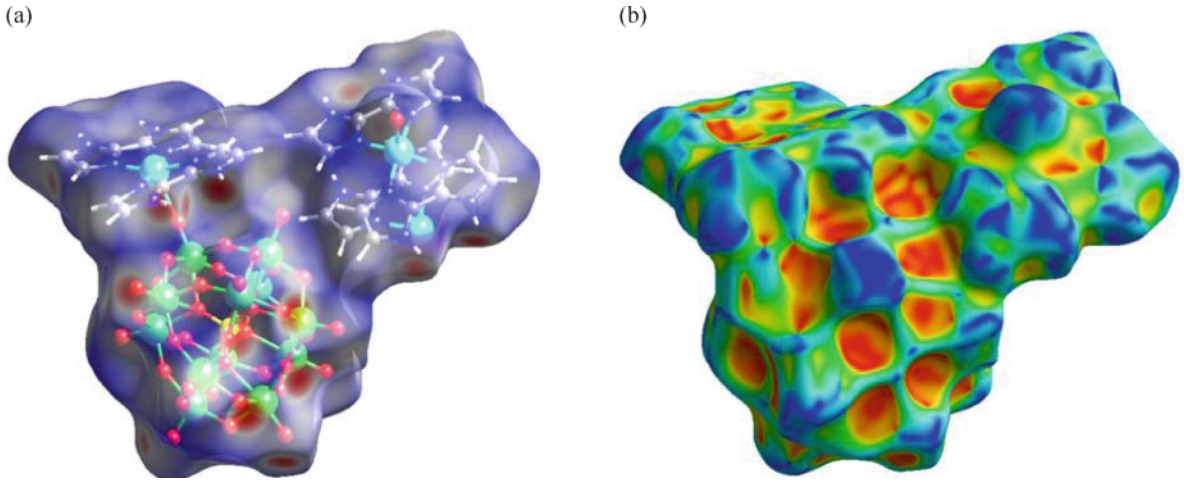

Fig. 2 (color online). Hirshfeld surface: (a) d_{norm} and (b) shape index for **1**.

respectively. For the $[Cu(2)(BIIM)_2(H_2O)]^{2+}$ ion at (x, y, z), N(11)–H and N(12)–H contact O(25) (x, $y+1$, z) and O(30) (x, y+1, z), and N(15)–H and N(16)–H interact with O(6) ($-x+1$, $-y$, $-z$) and O(2W) (x, y, z). For the $[Cu(3)(BIIM)_2]^{2+}$ ion at (x, y, z), N(19)–H and N(20)–H join O(26) (x, $y+1$, z) and O(27) (x, $y+1$, z). The components are thus linked by hydrogen bonds into a three-dimensional framework. There are also W–O$\cdots\pi$ interaction between the terminal oxygen atoms of the $[BW_{12}O_{40}]^{5-}$ anion and the imidazole ring, like for O(4) and the N(10) imidazole ring at ($x-1$, $y-1$, z) with a distance of 3.127(9) Å from O(4) to the ring centroid.

Hirshfeld surface analysis

Hirshfeld surfaces combing fingerprint plots generated by the CRYSTALEXPLORER 2.1 software [31] can identify the types and regions of intermolecular interactions and the proportion of this interaction to the total Hirshfeld surfaces area. Molecular Hirshfeld surfaces in crystal structures are constructed from the electron distribution. The normalized contact distances (d_{norm}) based on both d_e, d_i and the vdW radii of the atom are listed in Eq. 1. The 2D fingerprint plot is the combination of d_e and d_i [32, 33].

$$d_{norm} = \left(d_i - r_i^{vdW}\right)/r_i^{vdW} + \left(d_e - r_e^{vdW}\right)/r_e^{vdW} \quad (1)$$

Hirshfeld surfaces for **1** have been mapped over d_{norm} and the shape index (Fig. 2), respectively. The interactions between polyoxometalate oxygen and H atoms bonded to N atoms are shown as deep-red areas in the Hirshfeld surfaces. Pale-red areas on the surface correspond to weaker and longer contacts than hydrogen-bonding interactions. Visible spots are attributed to H$\cdots$H contacts. Obviously, a Hirshfeld surface can fully reflect the hydrogen bonding information listed in Table 3. The intermolecular N–H$\cdots$O (polyoxometalate and water) interactions with 56.7% contribution to the total Hirshfeld surface appear as two distinct spikes in the 2D fingerprint plots (Fig. 3a, b). The lower spike is attributed to O atoms interacting with H atoms bonded to nitrogen atoms, the upper spike being N–H atoms interacting with O atoms. O$\cdots$C/C$\cdots$O contacts constitute 3.9% (Fig. 3d) of the total Hirshfeld surface attributing to W–O$\cdots$C interactions, in which W–O(terminal oxygen)$\cdots\pi$(imidazole ring) appears in the fingerprint plots in a typical style. The scattered points spread up to $d_i = d_e =$ 1.0 Å correspond to H$\cdots$H interactions in the fingerprint plots (Fig. 3c). Obviously, there are no C–H$\cdots\pi$ interactions because there are no pairs of typical 'wings' at the top left and bottom right of the two-dimensional fingerprint plot. Moreover, π–π stacking interactions are not observed because the adjacent red and blue triangles do not appear in the shape index surface.

IR and UV spectra

The IR spectrum exhibits absorption peaks at 1425 – 1620 cm^{-1} which are associated with the BIIM

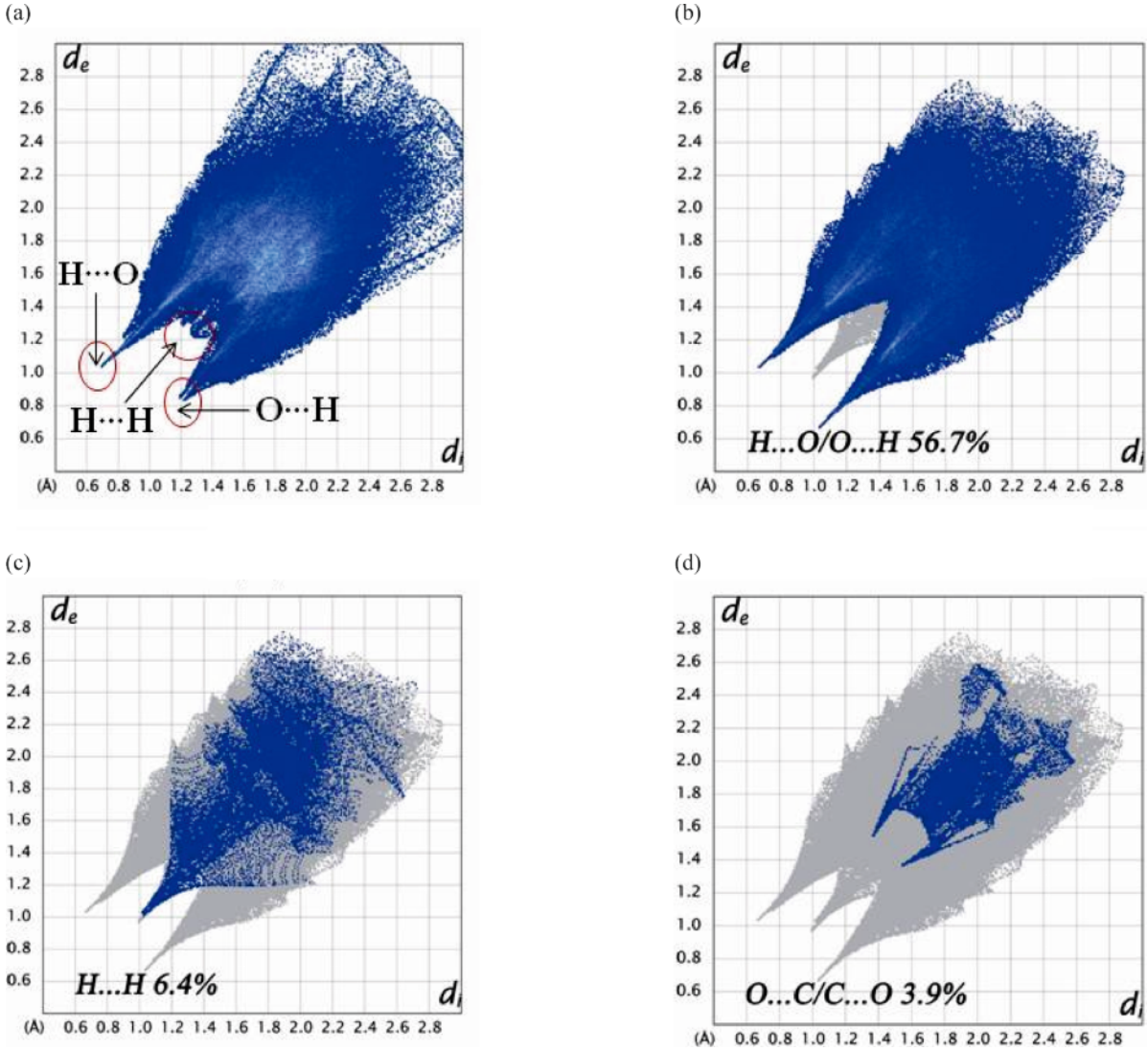

Fig. 3 (color online). Fingerprint plots: (a) full and involving (b) H···O/O···H, (c) H···H, and (d) O···C/C···O contacts showing the proportion of contacts contributing to the total Hirshfeld surface area of **1**.

Table 3. Hydrogen bond lengths (Å) and angles (deg) of **1**[a].

D–H···A	d(D–H)	d(H···A)	d(D···A)	∠DHA
N(3)–H(3A)···O(13)#2	0.86	2.16	2.995(12)	163.3
N(4)–H(4A)···O(16)#2	0.86	1.93	2.757(11)	161.3
N(7)–H(7A)···O(3W)	0.86	1.99	2.779(14)	152.3
N(8)–H(8A)···O(2)#3	0.86	2.16	2.846(12)	136.0
N(11)–H(11A)···O(25)#4	0.86	2.22	2.982(13)	147.4
N(12)–H(12A)···O(30)#4	0.86	2.00	2.813(11)	157.8
N(15)–H(15A)···O(6)#5	0.86	2.10	2.916(12)	157.3
N(16)–H(16A)···O(2W)	0.86	2.17	2.858(13)	137.3
N(19)–H(19A)···O(26)#4	0.86	1.85	2.649(11)	166.3
N(20)–H(20A)···O(27)#4	0.86	2.05	2.889(11)	165.2

[a] Symmetry codes: #2 $-x, -y+1, -z+1$; #3 $-x+1, -y, -z+1$; #4 $x, y+1, z$; #5 $-x+1, -y, -z$.

ligands. The band at 1000 cm^{-1} is characteristic of B–O stretching vibrations. The peak at 953 cm^{-1} corresponds to ν(W–O_t), and those at 906, 823, 755 cm^{-1} are attributed to ν(W–O–W). Compared with the IR spectrum of the parent α-Keggin cluster $H_5[BW_{12}O_{40}]$ [25], the characteristic vibrational frequencies for the compound have slightly shifted, affected mainly by the surrounding cations. The UV spectrum of **1** exhibits one intense absorption peak at 260 nm, which corresponds to the $O_{b,c}$→W charge transition. The O_t→W charge-transfer absorption band has disappeared because of the coordination mentioned above. This is characteristic of the Keggin-type polyanion.

Acknowledgement

This work was financially supported by the National Natural Science Foundation of China (21071043).

[1] M. T. Pope, *Heteropoly and Isopoly Oxometalates*, Springer, Berlin, **1983**.
[2] O. A. Kholdeeva, G. M. Maksimov, R. I. Maksimovskaya, M. P. Vanina, T. A. Trubitsina, D. Y. Naumov, B. A. Kolesov, N. S. Antonova, J. J. Carbo, J. M. Poblet, *Inorg. Chem.* **2006**, *45*, 7224.
[3] L. San Felices, P. Vitoria, J. M. Gutierrez-Zorrilla, L. Lezama, S. Reinoso, *Inorg. Chem.* **2006**, *45*, 7748.
[4] M. Sadakane, M. H. Dickman, M. T. Pope, *Angew. Chem. Int. Ed.* **2000**, *39*, 2914.
[5] P. Mialane, L. Lisnard, A. Mallard, J. Marrot, E. Antic-Fidancev, P. Aschehoug, D. Vivien, F. Secheresse, *Inorg. Chem.* **2003**, *42*, 2102.
[6] S. Reinoso, P. Vitoria, J. M. Gutierrez-Zorrilla, L. Lezama, L. San Felices, J. I. Beitia, *Inorg. Chem.* **2005**, *44*, 9731.
[7] M. Sadakane, Y. Iimuro, D. Tsukuma, B. S. Bassil, M. H. Dickman, U. Kortz, Y. Zhang, S. Ye, W. Ueda, *Dalton. Trans.* **2008**, 6692.
[8] X. L. Wang, C. Qin, E. B. Wang, Z. M. Su, Y. G. Li, L. Xu, *Angew.Chem. Int. Ed.* **2006**, *45*, 7411.
[9] Y. Y. P. Ren, X. J. Kong, X. Y. Hu, M. Sun, L. S. Long, R. B. Huang, L. S. Zheng, *Inorg. Chem.* **2006**, *45*, 4016.
[10] Q. G. Zhai, X. Y. Wu, S. M. Chen, Z. G. Zhao, C. Z. Lu, *Inorg. Chem.* **2007**, *46*, 5046.
[11] C. N. Kato, A. Shinohara, K. Hayashi, K. Nomiya, *Inorg. Chem.* **2006**, *45*, 8108.
[12] U. Kortz, *Inorg. Chem.* **2000**, *39*, 623.
[13] T. Yoshida, K. Nomiya, S. Matsunaga, *Dalton. Trans.* **2012**, *41*, 10085.
[14] F. J. Ma, S. X. Liu, C. Y. Sun, D. D. Liang, G. J. Ren, F. Wei, Y. G. Chen, Z. M. Su, *J. Am. Chem. Soc.* **2011**, *133*, 4178.
[15] M. G. Liu, P. P. Zhang, J. Peng, H. X. Meng, X. Wang, M. Zhu, D. D. Wang, C. L. Meng, K. Alimaje, *Cryst. Growth Des.* **2012**, *12*, 1273.
[16] A. X. Tian, J. Ying, J. Peng, J. Q. Sha, H. J. Pang, P. P. Zhang, Y. Chen, M. Zhu, Z. M. Su, *Inorg. Chem.* **2009**, *48*, 100.
[17] S. Reinoso, P. Vitoria, L. San Felices, A. Montero, L. Lezama, J. M. Gutierrez-Zorrilla, *Inorg. Chem.* **2007**, *46*, 1237.
[18] C. H. Zhang, Y. G. Chen, Q. Tang, S. X. P. Liu, *Dalton Trans.* **2012**, *41*, 9971.
[19] X. Y. Wu, Q. K. Zhang, X. F. Kuang, W. B. Yang, R. M. Yu, C. Z. Lu, *Dalton Trans.* **2012**, *41*, 11783.
[20] Y. Sawada, W. Kosaka, Y. Hayashi, H. Miyasaka, *Inorg. Chem.* **2012**, *51*, 4824.
[21] S. Li, D. Zhang, Y. Y. Guo, P. Ma, X. Qiu, J. Wang, J. Niu, *Dalton Trans.* **2012**, *41*, 9885.
[22] J. P. Wang, X. Y. Duan, X. D. Du, J. Y. Niu, *Cryst. Growth Des.* **2006**, *6*, 2266.
[23] H. Y. An, E. B. Wang, D. R. Xiao, Y. G. Li, Z. M. Su, L. Xu, *Angew. Chem. Int. Ed.* **2006**, *45*, 904.
[24] J. P. Wang, G. L. Guo, J. Y. Niu, *J. Mol. Struct.* **2008**, *885*, 161.
[25] J. W. Zhao, Y. P. Song, P. T. Ma, J. P. Wang, J. Y. Niu, *J. Solid State Chem.* **2009**, *182*, 1798.
[26] L. H. Wei, Z. L. Wang, J. W. Zhao, *Chin. J. Struct. Chem.* **2010**, *29*, 784.
[27] L. H. Wei, Z. L. Wang, M. X. Li, *Z. Naturforsch.* **2011**, *62b*, 1237.
[28] X. Fu, P. T. Ma, J. S. Wang, J. Y. Niu, *Russ. J. Coord. Chem.* **2010**, *36*, 622.
[29] G. M. Sheldrick, *Acta Crystallogr.* **2008**, *A64*, 112.
[30] A. L. Spek, *Acta Crystallogr.* **2009**, *D65*, 148.
[31] S. K. Wolff, D. J. Grimwood, J. J. McKinnon, D. Jayatilaka, M. A. Spackman, CRYSTALEXPLORER (version 2.1), University of Western Australia, Perth (Australia) **2007**.
[32] M. A. Spackman, J. J. McKinnon, *CrystEngComm* **2002**, *4*, 378.
[33] S. K. Seth, G. C. Maity, T. Kar, *J. Mol. Struct.* **2011**, *1000*, 120.